PHYSICAL AND MATHEMATICAL MODELING OF ACOUSTO-CONVECTIVE DRYING OF RICE

A. V. Fedorov,[a] **I. A. Fedorchenko,**[a] **S. B. An,**[b] **J. H. Lee,**[b] **and K. M. Choo**[c]

UDC 532.72;669.015.23

The present paper considers calculated and experimental data on acousto-convective drying of unhusked rice and analyzes the data on the drying of rise in three drying cells: in two installations of the Institute of Theoretical and Applied Mechanics (ITAM) of the Siberian Branch of the RAS — drying cells of small and medium cross-section — and in the large cross-section installation developed jointly by the Korea Polytechnic University and Doosan Co. LD. on the basis of the acousto-convective technology developed at the ITAM of the Siberian Branch of the RAS. In particular, calculated velocity distributions over the cell cross-section in the installation with a large cross-section are presented. The experiment has shown that the use of the two-mode acoustic signal for drying rice does not influence drying results as compared to the one-mode regime. The drying rate of rice placed in the audio-frequency generator chamber differed from the drying rate in the drying cell. The calculation method has been verified by the amplitude-frequency characteristics of the Hartmann generator.

Keywords: *acoustic drying of materials.*

Introduction. Acoustic drying of various types of materials received attention a few decades ago when it was discovered that the expenditure of energy and the drying time could be decreased significantly compared to the traditional convective method [1–3]. Below we present only a few studies devoted to these subjects. The phenomenon of water extraction under the action of an acoustic field from capillary materials such as wheat and corn was investigated in [4] at frequencies higher than 1 kHz. Experiments on drying green rice with the use of acoustic energy were carried out in [5] at 12–19 kHz. Apples and sweet potato cubes were tested at a frequency of 13 kHz in [6]. The influence of water activity on acoustic emission in wheat and rye bread was the subject of investigations in [7]. The best result in drying cylindrical pieces of potato was obtained in [8] at a frequency of 8100 Hz. Acoustic loudspeakers were used in air convective heating in [9].

At the ITAM of the Siberian Branch of RAS (Novosibirsk) a new method of acousto-convective drying of capillary materials was developed and realized [10–12]. In this method, to generate acoustic waves, the Hartmann generator was sued [13]. This generator, created at the beginning of the 20th century, is still one of the most effective methods for obtaining acoustic oscillations for media with a low acoustic conductivity. It is important that it can produce high-intensity single-mode oscillations in the air in a wide range of frequencies.

The Hartmann generator consists, as is known, of a convergent nozzle and a resonator with a piston. The resonator depth is an important factor in creating single-mode acoustic frequencies as is the distance between the nozzle exit and the edge of the resonator tube [14]. Some of the results of numerical simulations of acoustic waves generated by the jet flow into the resonator of the acousto-convective drier were presented in [15]. The mechanism by which acoustic oscillations increase the degree of drying is still not clearly understood. In the literature several theories explaining this phenomenon were proposed, for example, by R. M. G. Boucher in 1959 [16], Yu. Ya. Borisov and N. M. Gynkina [17], as well as by scientists from the ITAM of the Siberian Branch of the RAS [18, 19]. Thus, for gaining a better insight into the essence of the phenomenon, the numerical investigation of the processes of acousto-convective drying at different stages looks promising.

---

[a]Institute of Theoretical and Applied Mechanics, Siberian Branch of the Russian Academy of Sciences, 4/1 Institutskaya Str., Novosibirsk, 630090, Russia; email: irina@itam.nsc.ru; [b]Korean Polytechnical University, Sikhyn, South Korea; [c]Dooson Co. LTD, South Korea.
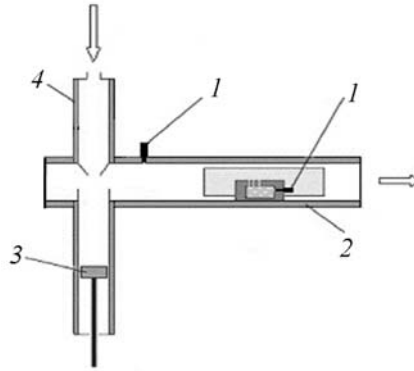
Fig. 1. Scheme of the part of the LCS installation for acousto-convective drying: 1) sensor; 2) drying cell; 3) piston; 4) converging nozzle.
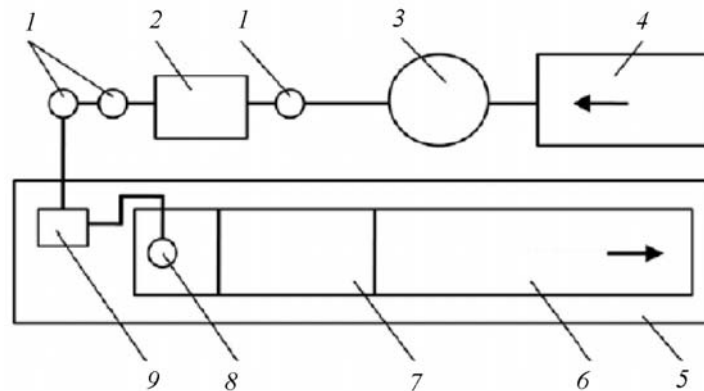

Fig. 2. Complete scheme of the LCS installation for acousto- convective drying: 1) filter; 2) drier; 3) reserve tank; 4) compressor; 5) container; 6) muffler; 7) drying cell; 8) converging nozzle; 9) pressure regulator.

In the present work, we have investigated by the methods of numerical simulation the nonstationary processes of flow of an air sonic jet into a submerged space, the impingement of the jet on the wall, and the injection of the jet into a resonator-limited space within the framework of various mathematical approaches, and with various formulations of the initial conditions. Here the resonator is a hollow cylinder with a closed end whose axis coincides with the axis of the jet. The cylinder diameter and the distance to the nozzle exit section are varied in the experiment in order to obtain different amplitudes and frequencies of acoustic oscillations.

Experimental Facility. Experiments on acousto-convective drying of capillary-porous materials have been carried out at the ITAM of the Siberian Branch of the RAS since the mid-1990s. In particular, in [18] the drying of wood was investigated by tomography methods. Here we will not touch on the drying of other materials [18–22] and will dwell on the results of drying unhusked Korean rice in the small (SCS — small cross-section) and medium (MCS — medium cross-section) installations of the ITAM of the Siberian Branch of the RAS obtained in 2007 [23] and in the large-scale (LCS — large cross-section installation) from South Korea. Figure 1 schematically represents the LCS acousto-convective drier developed jointly by the Korea Polytechnic University and the Doosan Co. LD., which is a scaled-up version of the installations of the ITAM of the Siberian Branch of the RAS [11].

In the experiments performed at the ITAM of the Siberian Branch of the RAS, two different types of acousto-convective driers were used: one drier with a small cross-section (52×52 mm) — SCS and the second drier with a medium size of the cross-section (200×200 mm) — MCS. In these driers, 0.05 and 10 kg of rice, respectively were dried [23]. It turned out that a change in the weight of the rice being dried by two orders of magnitude does not lead to a change in the drying rate, i.e., the scale factor is absent. In these experiments, we used, as a container for the portion of rice to be dried int he SCS drier, a fine-pore nylon sack. We placed in the MCS drier rectangular drying cartridges ($180 \times 1000 \times 50$ mm), setting them perpendicularly to the generator axis. The angle between the cartridge
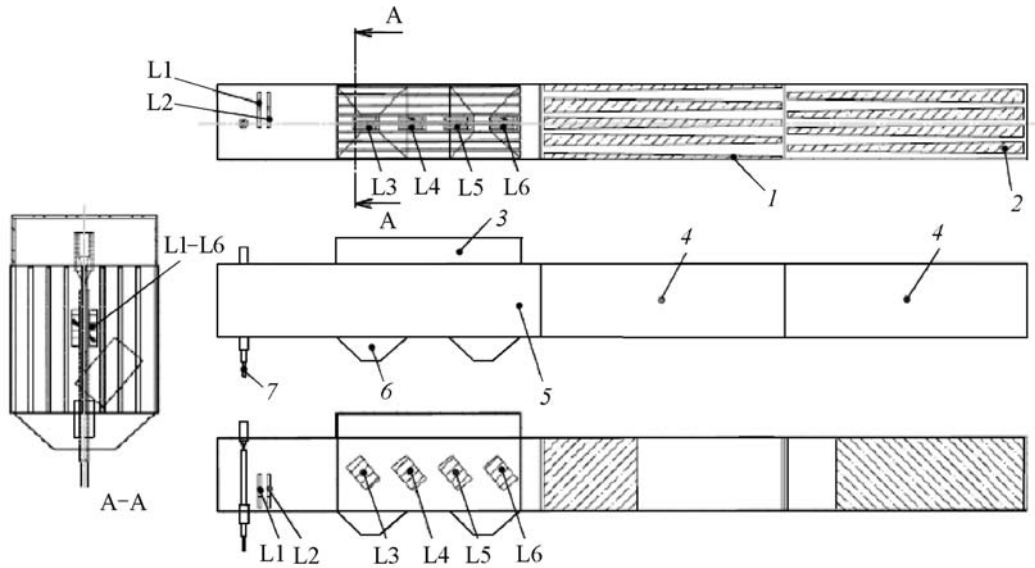
Fig. 3. Location diagram of packets in the LCS experiment: 1) lateral part of the noise gasket; 2) central part of the noise gasket; 3) top; 4) muffler case; 5) case; 6) bottom; 7) piston.
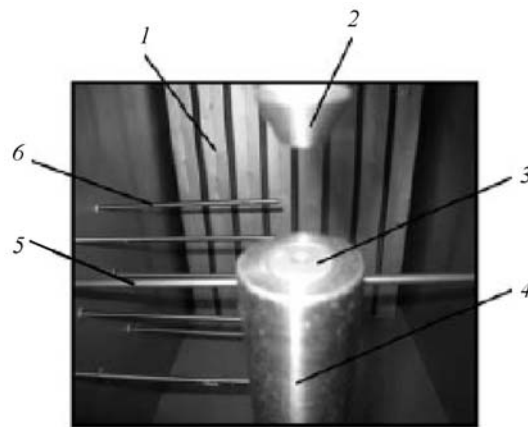

Fig. 4. Interior of the LCS installation: 1) cartridge for storing rice; 2) converging nozzle; 3) resonator piston; 4) resonator cylinder; 5) multipurpose velocity and pressure transducers and temperature sensor; 6) temperature sensor.

and the nozzle is an important factor for effective drying [10, 24, 25]. The frequencies for the SCS and MCS installations were equal to 415 and 130 Hz, respectively, and the sound pressure level was the same, 167 dB. The generator frequency was selected by varying the distance between the nozzle and the resonator end. Although the pressure, density, and velocity in different regions of the driers had different values, the best results for both driers turned out to be very close.

To explore the possibilities of using the acousto-convective drying technology in industrial applications, we carried out experiments in the LCS installation with a large volume of rice to be dried. The volume of the drier in this installation is 500 times that in the MCS one, i.e., it is designed for 200 kg. The sizes of the Hartmann generator therewith in both driers are close. Figure 2 schematically represents the LCS installation for acousto-convective drying.

In the course of experiments, two of the six cloth sacks intended for loading the material, were placed in the sound production chamber, and the other four sacks were placed in the drying cell. The arrangement of these cloth packets in the LCS experiments is given in Fig. 3.
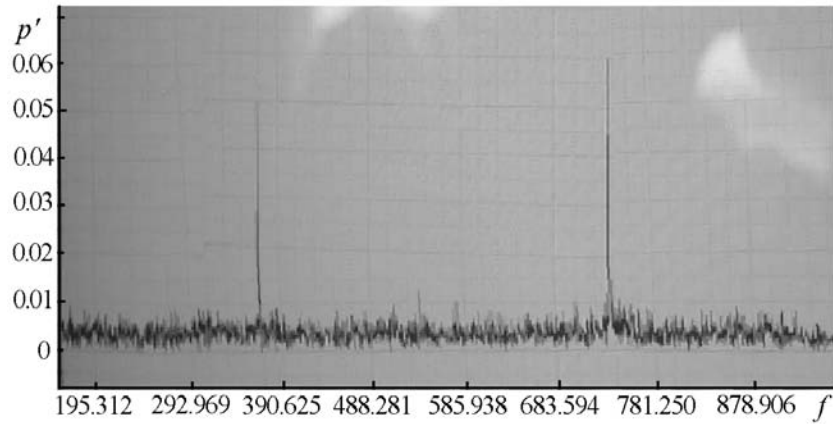
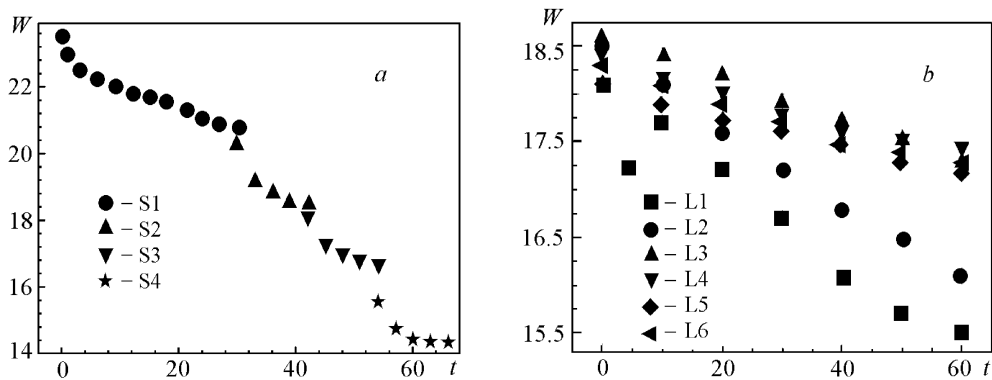Fig. 5. Frequency spectrum in the LCS installation.

Fig. 6. Comparison between the experimental results on the moisture content distribution with time: a) installation of the ITAM of the Siberian Branch of the RAS; 6) South-Korean installation. W, %; t, min.

The drying procedure in the LCS included preparation of samples of the material (rice) to be dried, measurement of their weight before and after the experiment, and storage of the sample in vinyl bags during each experiment. The interior of the LCS installation for convective drying is shown in Fig. 4. The instruments for temperature, velocity, and pressure measurements were located at 12 points. The photograph given in this figure shows nine points for measurements on the left wall. It turned out that at the given geometric parameters of the installation and the Hartmann generator in the LCS, two-mode sound generation takes place (Fig. 5).

Before the experiment in the MCS installation, the initial moisture content of rice in the storage was 13–15%. Upon adding water and holding in the refrigerator for 24 h, the final moisture content was 22.4–24.3%, For experiments in the LCS installation, the initial moisture content of rice was 14%, and the final moisture content under the same conditions was 18.1–18.6%. The moisture content of the rice shell and rice was measured by means of a grain moisture tester (KETT, PQ-510, Japan). The atmospheric humidity was measured by a hygrometer (TES, 1365, Taiwan). It was assumed that the supplied moisture penetrated not only into the shell but also into the grains of rice. The quantity of rice being dried and the position of the container with rice in the experiments in chambers with different sizes differed. In the case with the SCS, a container with 0.05 kg of rice was placed at the end of the drying cell. For the SCS, the mass of rice being dried was 4.2 kg (six sacks with 700 g of rice each), and packets with rice were located in six different positions in the installation.

In the MCS drying cell, the complete cycle of rice treatment consisted of six 10-min drying sessions with 30-min drying intervals, during which hardening of the rice took place [19, 23]. Hardening, as we call it, is the settling time of the portions of rice dried outside the drying cell. Hardening is carried out in the room at the same temperature as in the drying cell (298 K).
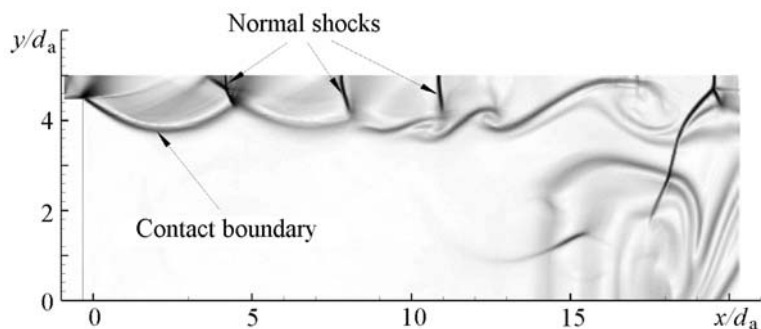
75

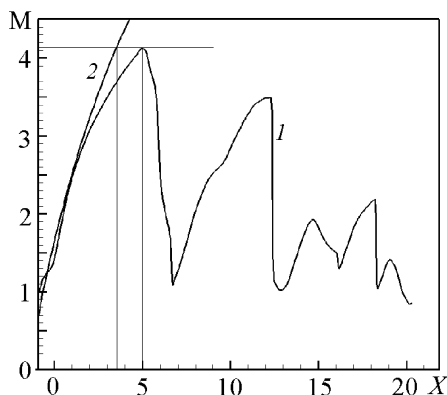Fig. 7. Numerical flow schlieren-pattern of the submerged jet.

Fig. 8. Mach number distribution along the symmetry axis: 1) calculation; 2) empirical formula of [27]. $X = x/d_a$.
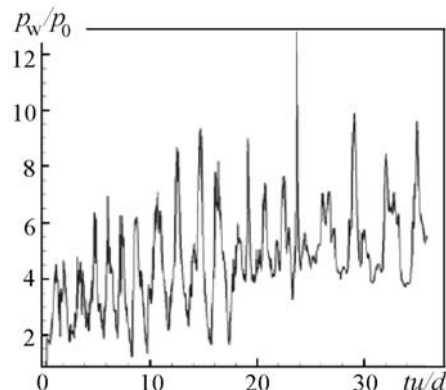
Fig. 9. Wall pressure distribution on the jet axis as a function of dimensionless time.

The complete process of drying in the LCS took 4,384 min: four 10–30-min drying periods and three hardening periods 1440 min each carried out inside the refrigerator. The rice was stored in separate vinyl packets protecting it from moistening and drying out during the hardening process, which is important under variable atmospheric conditions.

Experimental Results. Although the experimental conditions for the MCS and LCS installations were different, the results point to the existence of the same physical mechanism of the phenomenon. The process of water extraction in the LCS is the fastest in the packet L1 (taking 60 min) located closest to the nozzle. The average gas velocity in the MCS is 22 m/sec, which corresponds to the average velocity of the flow near the rice surface. For the LCS, the gas velocity was about 1 m/sec. The average velocity near the rice surface in the process of acousto-convective drying is one of the most important parameters. Figure 6 shows the data on the drying kinetics (S1–S4 are the stages of the drying process, L1–L6 are the positions occupied by the packets in the LCS installation). As is seen, for different positions of the containers the drying process is different. In the drying cell channel the drying process is uniform. Note that the drying curves for L3–L6 are similar; at the same time near the acoustic energy source more intensive drying takes place (see L1, L2).

Results of the Two-Dimensional Modeling. *Numerical method.* To calculate laminar jet flows, we used an original two-dimensional numerical algorithm based on complete Navier–Stokes equations developed at the ITAM of the Siberian Branch of the RAS [26]. For numerical approximation of the transfer terms, we used a TVD approach based on the van Lear flow vector separation method and a central finite-difference scheme for approximately viscous terms. A four-step implicit scheme of the first order of accuracy was used for time-interpretation.

Flow into a submerged space. At the first stage of investigations, in order to verify the mathematical model and the numerical algorithm in solving problems including the flows of underexpanded jets, the problem on the flow of an air sound sonic jet into a submerged space was calculated. Modeling in the laminar approximation made it possible to determine the main characteristics of the flow. The numerical schlieren photograph of the process of jet flow
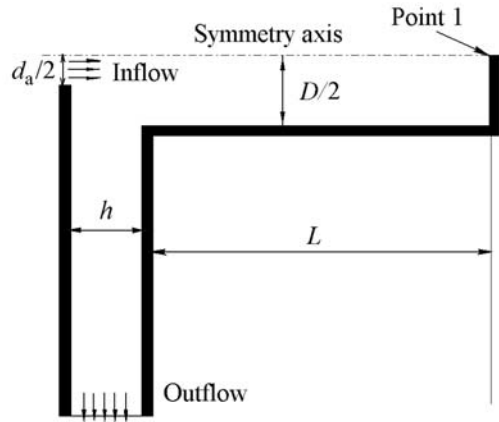
Fig. 10. Scheme of the resonator problem.

into stationary air under normal conditions is shown in Fig. 7. The upper boundary is the symmetry axis of the flow. The spatial variables were dedimensionalized to the diameter of the nozzle exit section. It is easy to distinguish all the main structures characteristic of underexpanded jets: the contact surface of the jet and the transverse shock waves forming the periodic multibarrel structure of the flow.

For quantitative comparison of the flow characteristics the Mach number distribution on the symmetry axis obtained from the calculations was compared with the empirical distribution [27] along the length of the first barrel. As can be seen from Fig. 8, there is a good agreement among the data. Vertical lines show the calculated and the empirically predicted value of the length of the first barrel.

Interaction of the sonic jet with an infinite barrier. The second stage of investigations was the calculation of the interaction between the jet and a solid wall, which was also carried out on the basis of luminary flow equations. It is known that such a type of interaction may lead to the appearance of a global instability of the flow, which depends on the distance between the nozzle exit section and the wall and the incalculability of the jet. Calculations were performed for a distance to the wall equal to 14 diameters of the nozzle exit section at an incalculability of the jet of 3.47. The time dependence of the wall pressure distribution on the jet axis is shown in Fig. 9. According to the empirical relation proposed in [28], the vibration frequency of the jet is estimated to be 380 Hz. With the use of the Fourier transform for the pressure distribution obtained from the present calculation, it has been found that the prevailing vibration frequency is about 500 Hz. The difference between the numerical and empirical results may be due to the two-dimensional geometry of the calculation domain.

Flow in the resonator. The problem on the jet flow into the resonator was investigated in the two-dimensional formulation on the basis of laminar Navier–Stokes equations. The scheme of the formulation problem is given in Fig. 10. In the left inlet cross-section at a distance of a half of the nozzle diameter, the following conditions were given: M = 1, static temperature of 250 K, static pressure of 2.915 atm. On the symmetry axis, reflection conditions for the vertical velocity component and a zero gradient of all the other parameters were given. In the outlet (lower) cross-section, the condition of equality to zero of the gradient of all quantities and at all the other boundaries the adhesion conditions were used. The outlet cross-section was chosen at a fairly long distance from the inlet one in order to hold constant the incalculability coefficient of the jet. In [29], it was shown that such conditions permit satisfying the given requirement.

The instantaneous flow field realized for the case of $h = 2d_a$ and $L = 17d_a$ is given in Fig. 11a. This geometry of the resonator corresponds to the sizes of the Hartmann generator used in the drying cell of the MCS installation. The normal shock resulting from the underexpanded nature of the jet moves periodically forward and back along the jet axis. Compression waves propagate inside the resonator and are reflected from its closed end. Part of the mass flow of the jet gets into the resonator and part does not, since a high pressure is created there due to the multiple reflection of compression waves from the tube end. As a result, because of the counterflows and the high pressure inside the resonator tube, the flow velocity there is not high. Some of the vortex structures arising inside the channel can be seen in Fig. 11b where the streamlines for the same instant of time as for Fig. 11a are shown. At a distance of about
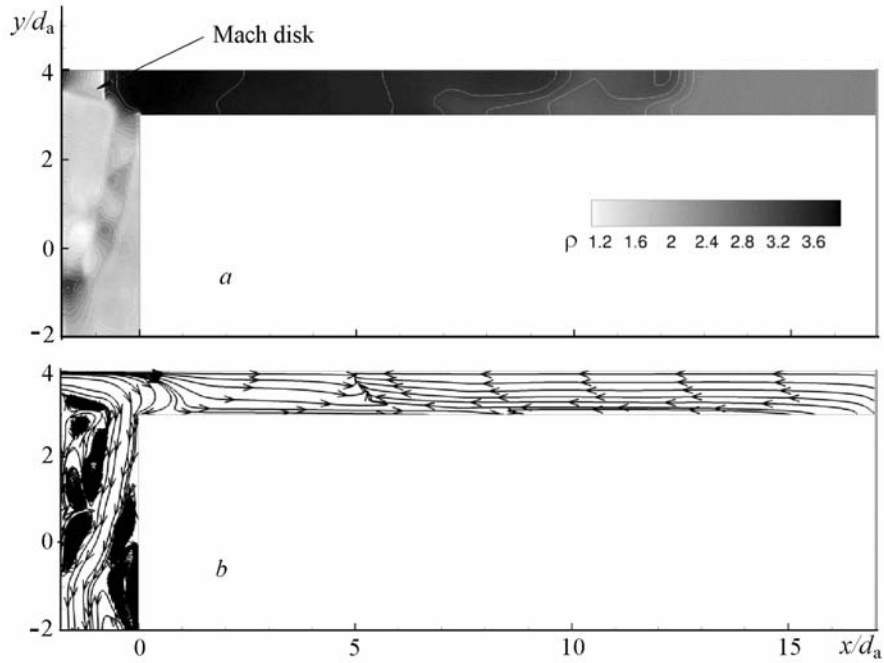
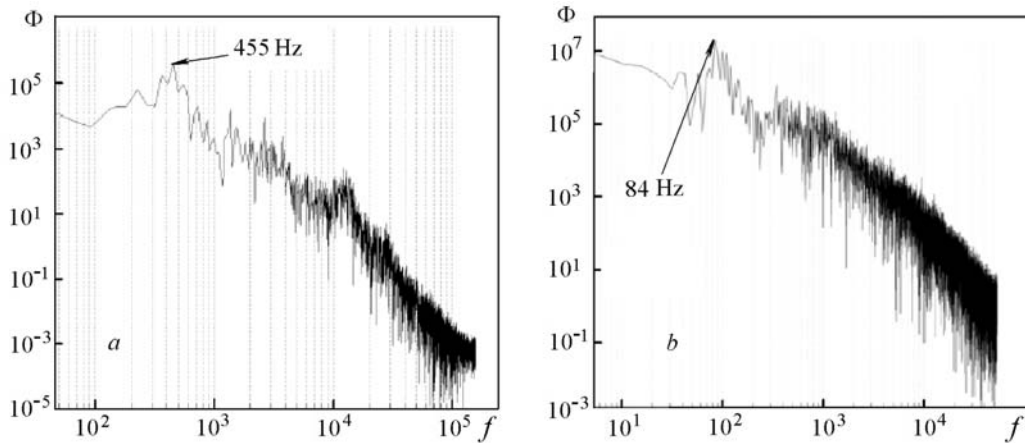Fig. 11. Instantaneous density field (a) and instantaneous streamlines (b). ρ, kg/m^3.

Fig. 12. Spectral energy density at point 1: a) SCS; 2) MCS. f, Hz; Φ, Pa^2.

$x/d_a = 5$ one can see the meeting line of two flows moving in opposite directions. From the calculations we obtained the pressure distribution at point 1 (see Fig. 10) and plotted its Fourier transform. The fundamental frequency turned out to be equal to 455 Hz, as is shown in Fig. 12a. The experimental value of 415 Hz is in good agreement with the predicted result.

An analogous numerical investigation has also been carried out for the installation of large geometric sizes at $L = 19.8d_a$ and $h = 2.67d_a$. In this case, the predicted acoustic frequency of the process is 84 Hz (Fig. 12b). The experimental value for the MCS installation where $h = 6.67d_a$ at the same resonator depth is 130 Hz. Thus, the difference between the numerically predicted and the experimental value of the frequency is due to the difference in the problem geometry, as well as to the simplifications in the calculations concerning the two-dimensionality of the flow. The calculation of a Hartmann generator with a longer distance from the nozzle to the resonator requires large computational resources and will be carried out later.

The instantaneous distribution of the vertical velocity in the outlet channel of the MCS installation in its four different cross-sections is given in Fig. 13. As can be estimated, the velocity in the lowest calculated cross-section
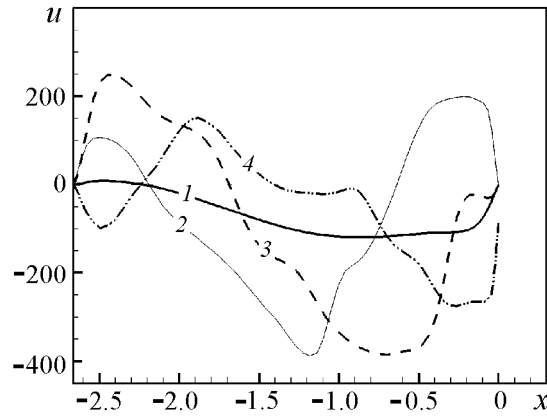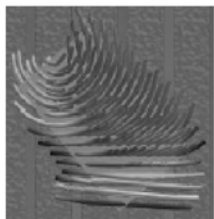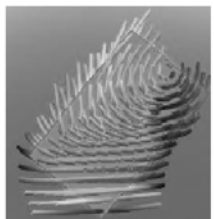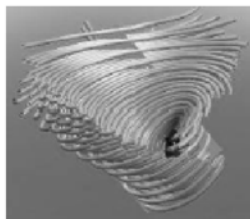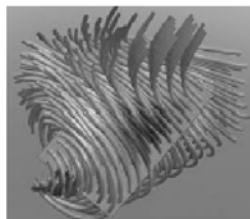
Fig. 13. Velocity distribution in the outlet channel cross-sections: 1) at a distance of 14.3 diameters from the symmetry axis; 2) 3.6 nozzle diameters; 3) 2.3 diameters; 4) 1.1 diameters. The coordinate x has been dedimensionalized to the nozzle diameter. u, m/sec.

TABLE 1. Modeling Results for Packets L1 and L5 in the LCS Installation

Packet number	L1		L5	
View	Front	Rear	Front	Rear
Velocity isoline				
Minimum value	2.667	2.656	0.100	0.145
Maximum value	8.032	8.063	0.970	0.966
Average value	5.349	5.359	0.535	0.555

does not exceed 150 m/sec, and the average flow velocity is 70 m/sec. Estimating calculations show that when the size of the outlet cross-section is increased to the experimental one, then the velocity is 28 m/sec, which is close to the value obtained experimentally.

Results of the Three-Dimensional Modeling. The table presents the results of the numerical simulation of the flow in the LCS installation performed at the Korea Polytechnic University for sacks L1 and L5. The isolines show the velocity values at time 0.3 sec for each packet of rice. Radically different phenomenon taking place on the surface of the sacks can be observed. On the surface of sack L5 there are large vortex rings, which leads to excessive energy losses in the drying process. These vortices arise because of the sharp increase in the volume of the drying cell caused by the flow from the generator chamber into the drying compartment. The backflow from the muffler walls pressing back the incoming flow also has an effect. Thus, the use of an open channel is not optimal.
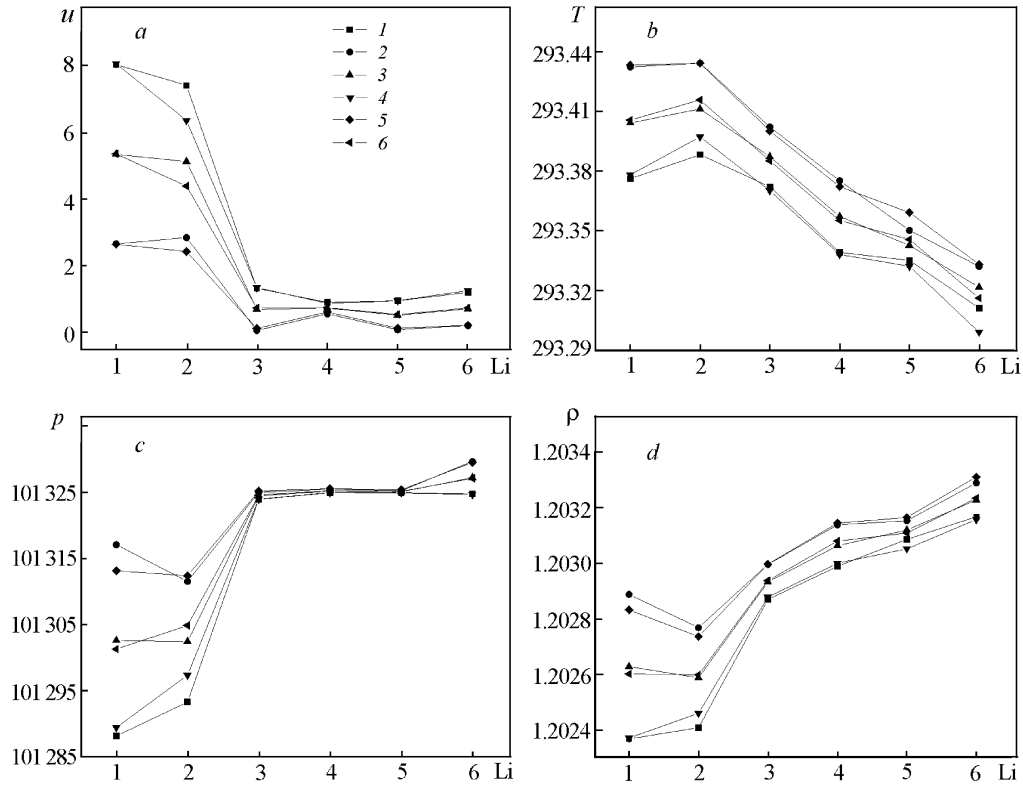
Fig. 14. Behavior of the minimum (1, 4), maximum (2, 5), and average (3, 6) values of parameters depending on the location of packets: 1–3) front part of the sack; 4–6) rear part of the sack. u, m/sec; T, K; p, Pa; ρ, kg/m^3.

Sack L6 is also subjected to the action of the backflow from the muffler walls. The gap between the end of the drying cell and the open end of the muffler must be large enough so that no appreciable counterpressure on the barriers is produced. The velocity isolines are given in the table since its distribution plays a key role in the drying process. All the other parameters are given in less detail. Figure 14 shows the behavior of the maximum, minimum, and mean values of four different parameters on the front and rear parts of each of the rice sacks L1–L6. Here on the abscissa the number of the packet being dried and on the ordinate the dynamic and thermodynamic parameters of the gas near the packets are plotted. It is useful to see what values of the velocity, temperature, pressure, and density parameters arise in the vicinity of each packet depending on its position. Packets L1 and L2 in the generator show a higher drying efficiency than packets L3–L6 in the drying cell. In general, packets L1 and L2 are influenced by the flow having a higher velocity to a greater extent than packets L3–L6, which may be a reason for the faster extraction of water. The behavior of the other parameters such as the temperature, the pressure, and the density is similar for all packets L1–L6.

CONCLUSIONS

1. We have presented the data of the experimental-theoretical investigation of acousto-convective drying in drying cells of medium and large sizes showing that in both installations (MCS and LCS) similar mechanisms of the process of acousto-convective drying of unhusked Korean rice are observed.

2. Mathematical models have been developed on the basis of Navier–Stokes equations for describing the gas flows in the channels of the medium and large installations verified by the amplitude- frequency characteristics of the gas flow process.

3. It has been shown that the use of one- and two-mode operation of the drying cell does not lead to a wide difference between the characteristics of the process of acousto-convective drying of rice.

NOTATION

d_a, diameter of the critical cross-section of the nozzle, m; D, resonator diameter, m; f, frequency, Hz; h, width of the outlet channel of the drying installation, m; L, resonator length, m; M, Mach number; p, pressure, Pa; p', sound signal amplitude, mV; t, time, min; u, velocity, m⁄sec; W, relative humidity; x, longitudinal coordinate, m; y, transverse coordinate, m; ρ, density, kg⁄m^3; Φ, spectral energy density, Pa^2. Subscripts: 0, undisturbed flow parameters; a, parameters on the nozzle exit section; w, parameters on the wall.

REFERENCES

1. A. V. Luikov, *Theory of Drying* [in Russian], Énergiya, Moscow (1968).
2. R. S. Soloff, Sonic drying, *J. Acoust. Soc. Am.*, **36**, No. 5, 961–965 (1964).
3. A. V. Fedorov and V. M. Fomin, Physicomathematical modeling of the phenomenon of acoustoconvective drying, in: *Heat and Mass Transfer–MIF-2008: 6th Minsk Int. Forum* [in Russian], May 19–23, 2008, Vol. 1, Minsk (2008), pp. 45–46.
4. C. C. Huxsoll and C. W. Hall, Effects of sonic irradiation on drying rates of wheat and shelled corn, *ASAE*, **13**, 21–24 (1970).
5. S. H. Muralidhara and D. Ensminger, Acoustic Drying of Green Rice, *Drying Technol.*, **4**, No. 1, 137–143 (1986).
6. R. A. Carlson, D. F. Farkas, and R. M. Curtis, Effect of sonic energy on the air drying of apple and sweet potato cubes, *J. Food Sci.*, 37, 793–794 (1972).
7. A. Marzec, P. Lewicki, and Z. Ranachowski, Influence of water activity on acoustic emission of flat extruded bread, *J. Food Eng.*, **79**, 410–422 (2007).
8. L. G. Bartolome, J. E. Hoff, and K. R. Purdu, Effect of resonant acoustic vibrations on drying rates of potato cylinders, *Food Technol.*, **23**, No. 3, 47–50 (1969).
9. D. E. Scarborough, R. I. Sujith, and B. T. Zinn, The effect of resonant acoustic oscillations on heat and mass transfer rates in a convection air dryer, *Drying Technol.*, **24**, No. 8, 931–939 (2006).
10. V. N. Glaznev, Yu. G. Korobeinikov, and N. V. Terpugov, Extraction of water from a capillary sample in an acoustic field, *Inzh.-Fiz. Zh.*, **73**, No. 4, 686–687 (2000).
11. Yu. G. Korobeinikov, A. V. Fedorov, and V. M. Fomin, A method for drying materials and a device for its implementation, Patent No. 2270966 (2006).
12. Yu. G. Korobeinikov, A. P. Petrov, G. A. Trubacheev, and A. V. Fedorov, Investigation of the process of drying a capillary sample subjected to an acoustic-convective effect, *Inzh.-Fiz. Zh.*, **80**, No. 2, 166–172 (2007).
13. J. Hartmann, On a new method for the generation of sound waves, *Phys. Rev.*, **20**, 719 (1922).
14. V. N. Glaznev and Yu. G. Korobeinikov, *The Hartmann effect. The existence domain and vibration frequencies*, *Zh. Prikl. Mekh. Tekh. Fiz.*, **42**, No. 4, 62–67 (2001).
15. A. V. Fedorov, N. N. Fedorova, I. A. Fedorchenko, Yu. G. Korobeinikov, K. M. Choo, S. B. An, and H. J. Lee, Numerical simulation of acoustic waves in jet flows, in: *Book of Abstracts of 5th Int. Conf. on Computational Fluid Dynamics*, Seoul (2008).
16. R. M. G. Boucher, Drying by airborne ultrasonics, *Ultrasonics News*, **3**, 8–16, (1959).
17. Yu. Ya. Borisov and N. M. Gynkina (L. D. Rozenberg Ed.), *Physical Principles of Ultrasonic Technology* [in Russian], Nauka, Moscow (1970), pp. 580–640.
18. V. N. Glaznev, I. V. Koptyug, and Yu. G. Korobeinikov, Physical features of acoustic drying of wood, *Inzh.-Fiz. Zh.*, **72**, No. 3, 437–439 (1999).
19. Yu. G. Korobeinikov, A. P. Petrov, and A. V. Fedorov, Visualization of the process of water extraction from transparent model samples in convective and acoustic drying, *Inzh.-Fiz. Zh.*, **77**, No. 2, 31–35 (2004).
20. Yu. G. Korobeinikov, A. A. Nazarov, and A. V. Fedorov, Energy expenditures in drying wood by acoustic technique, *Derevoobrab. Promysh.*, No. 4, 6–7 (2004).
21. Yu. A. Gosteev, Yu. G. Korobeinikov, A. V. Fedorov, and V. M. Fomin, Investigation of the warming-up of model samples in acousto-convective drying, *Zh. Prikl. Mekh. Tekh. Fiz.*, **46**, No. 5, 116–122 (2005).

22. Yu. G. Korobeinikov, A. P. Petrov, G. A. Trubacheev, and A. V. Fedorov, Thermal effects in model samples in acousto-convective drying, *Inzh.-Fiz. Zh.*, **79**, No. 2, 168–173 (2006).

23. Yu. G. Korobeinikov, G. A. Trubacheev, A. V. Fedorov, K. M. Chu, D. M. Zheong, and Yu. I. Kim, Experimental investigation of the acousto-convective drying of unhusked Korean rice, *Inzh.-Fiz. Zh.*, **81**, No. 4, 652–655 (2008).

24. Yu. G. Korobeinikov and A. V. Fedorov, On the extraction of water from a capillary sample in an acoustic field, *Inzh.-Fiz. Zh.*, **76**, No. 1, 7–10 (2003).

25. Yu. G. Korobeinikov, A. P. Petrov, G. V. Trubachev, and A. V. Fedorov, Investigation of the process of drying a system of connected capillaries in an acoustic-convective field, *Inzh.-Fiz. Zh.*, **81**, No. 6, 1097–1101 (2008).

26. A. V. Borisov and N. N. Fedorova, Calculation of turbulent detached flows on the basis of the method of higher-order approximation, *Teplofiz. Aéromekh.*, **2**, No. 3, 253–269 (1995).

27. V. G. Dulov and G. A. Luk'yanov, *Gas Dynamics of Outflow Processes* [in Russian], Nauka, Novosibirsk (1984).

28. B. G. Semiletenko, B. N. Sobkolov, and V. N. Uskov, Approximate calculation of the amplitude-frequency characteristics of unstable interaction of a supersonic jet with a normally fixed flat obstacle, *Izv. SO Akad. Nauk SSSR*, **3**, No. 13, 34–39 (1975).

29. V. E. Kuz'mina and S. K. Matveev, On the numerical investigation of unstable interaction of a supersonic jet with a flat obstacle, *Zh. Prikl. Mekh. Tekh. Fiz.*, **20**, No. 6, 732–737 (1979).